JOURNAL OF THERMOPHYSICS AND HEAT TRANSFER
Vol. 9, No. 1, January–March 1995

Comparison of Discrete Ordinates Formulations for Radiative Heat Transfer in Multidimensional Geometries

W. A. Fiveland* and J. P. Jessee†
Babcock & Wilcox, Alliance, Ohio 44601

This article compares predictions of radiative heat transfer in two-dimensional enclosures for several formulations of the discrete ordinates method. The discrete ordinates equations are formulated for an absorbing, isotropically scattering, and re-emitting medium enclosed by gray walls. Control volume based finite element formulations of the radiative transport equation (RTE) are presented for the primitive variable (PV) and even parity (EP) equations. These formulations are compared to the finite element formulation of the EP equations, to the control volume formulation of the PV radiative transport equation, and to exact solutions. Several test enclosures are modeled, including enclosures with either absorbing or isotropically scattering media. Solution accuracy is investigated for two angular discretization schemes: 1) the S_n discrete ordinates approximation and 2) the piecewise constant angular approximation. The PV formulations of the RTE appear to be more accurate than EP formulations.

Nomenclature

E_b = emissive power, $\bar{\sigma}T^4$, W/m^2
G = incident energy, $\int_{4\pi} I\, d\Omega$, W/m^2
G^* = nondimensional incident energy, G/E_b
I = intensity, $I(\boldsymbol{r}, \boldsymbol{\Omega})$, W/m^2·sr
M = total number of discrete ordinate directions
N = total number of global nodes
N_i = basis function
N_θ = number of divisions in polar direction
N_ϕ = number of divisions in azimuthal direction
n = surface normal
Q^* = nondimensional net wall heat flux, q/E_b
q = heat flux, $\int_{2\pi} |\boldsymbol{n}\cdot\boldsymbol{\Omega}| I\, d\Omega$, W/m^2
R = radius, m
$\boldsymbol{r}$ = position vector, m
S_m = in-scattering source term, W/m^3-sr
S_n = order of discrete ordinates approximation
w = weight function
w_m = direction weights
x, y, z = coordinate directions, m
x^*, y^*, z^* = nondimensional coordinates, x/L, y/L, z/L
β = extinction coefficient, m^{-1}
Γ = boundary of domain, Λ
ε = emissivity
ζ = generic direction cosine
θ = polar angle
κ = absorption coefficient, m^{-1}
Λ = domain
μ, ξ, η = direction cosines
ρ = reflectivity, 1-ε
σ = scattering coefficient, m^{-1}
$\bar{\sigma}$ = Boltzmann's constant, W/m^{-2} K^{-4}
ϕ = azimuthal angle
ψ = average intensity, W/m^2-sr
$\boldsymbol{\Omega}$ = direction with direction cosines, μ, ξ, η

Subscripts
b = blackbody
m = direction
n = nth S_n approximation

Superscripts
$'$ = incoming direction
$*$ = nondimensional value
$\hat{}$ = unit vector

Introduction

CONSIDERABLE attention has recently been focused on developing accurate methods of solving the radiative transport equation (RTE) for multidimensional geometries. Viskanta and Menguc[1] and recent text[2] extensively review the available methods of solving the RTE for participating media. The discrete ordinates method has been widely applied[3–7] because it has several desirable features: the method is relatively easy to code, it requires a single formulation to invoke higher-order approximations, and it integrates easily into control volume transport codes.

A number of variations of the discrete ordinates method have been presented in the last decade. Originally, the discrete ordinates method was developed to solve the RTE for neutron transport applications by Lathrop and Carlson.[8] Later, the method was developed for radiative heat transfer by Fiveland,[3–5] Truelove,[9] Kim and Lee,[6] and Jamaluddin and Smith.[7] These methods, which are based on a transport equation in terms of the radiant intensity, are termed primitive variable (PV) formulations.

The even parity (EP) form of the transport equation[10] has been solved with the discrete ordinates method for both neutron transport applications[10,11] and radiative heat transfer applications.[12] These works used finite element spatial discretizations and strict discrete ordinates angular discretizations. The EP form has the following advantages over the PV formulations of Ref. 4 and others:

1) Physically unrealistic negative intensities of the PV formulation and the corresponding "flux fix-ups"[3–5,13] are avoided, since the EP equations are positive definite and self-adjoint.[11]

2) Spatial discretization is simplified because the second-order EP equations do not exhibit the one-way characteristics of the first-order PV equations. Consequently, standard spatial discretization schemes and linear equation solvers from convective transport flow codes may be readily applied to radiative heat transfer.

Received Feb. 18, 1994; revision received Sept. 12, 1994; accepted for publication Sept. 19, 1994.

*Manager, Numerical Modeling Section, Research and Development Division. Member AIAA.
†Research Engineer, Numerical Modeling Section, Research and Development Division. Member AIAA.

For some problems, nevertheless, the even parity form has produced solutions with inferior accuracy compared to the primitive variable forms,[12] triggering the need for a closer investigation of the various formulations.

In addition, a number of spatial differencing schemes and ordinate sets have been used by workers for the primitive variable formulation. Differencing schemes have included the step, diamond difference, positive, variable-weight, and exponential schemes. Unfortunately, none of these schemes seem to be completely satisfactory: the step scheme is lower-order and highly dispersive; the diamond difference, positive, and exponential schemes may produce negative or oscillatory solutions; and the variable-weight scheme sacrifices accuracy to obtain bounded solutions.

From an angular differencing standpoint, the standard S_n approximation has been the most commonly used method. The selection of directions and weights is detailed in Ref. 14. In attempts to mitigate the well-known ray effects of the S_n approximations, a number of workers[15-17] have employed methods similar to the piecewise constant angular (PCA) approximation.[18] While the PCA approximation mitigates ray effects, it does not necessarily conserve a number of key moments of the radiant intensity.

This article presents a comparison of several forms of the discrete ordinates method for radiative heat transfer. Control volume based, finite element (CVFEM) discretizations of the primitive variable (PV-CVFEM) and even parity equations (EP-CVFEM) are derived. To overcome problems with conventional spatial differencing schemes, the bounded, second-order MINMOD scheme[19] is implemented in the PV-CVFEM formulation. Two angular discretization schemes—1) the strict discrete ordinates (DO) approximation and 2) the piecewise constant angular (PCA) approximation—are considered. Predictions are made for several test enclosures with absorption and scattering. The present formulations are compared to 1) the standard control volume discrete ordinates method[3-5] (PV-CV) and 2) the even parity, finite element method (EP-FEM).[12] The cases contrast the EP and PV equations, the S_n and PCA angular approximations, and the diamond difference and MINMOD spatial-differencing schemes.

Although cases are presented for gray and isotropically scattering media, all formulations may be extended to nongray and anisotropically scattering media as shown by Fiveland and Jamaluddin[5] and Fiveland,[4] respectively. For anisotropically scattering, the EP formulations require the addition of the odd parity equations.[10]

Analysis

Governing Equations

Consider the radiative transfer equation for the region Λ, shown in Fig. 1. The balance of energy passing in a specified direction $\boldsymbol{\Omega}$ through a small differential volume in the emitting-absorbing and isotropically scattering gray medium can be written as follows:

$$(\boldsymbol{\Omega}\cdot\nabla)I(\boldsymbol{r},\boldsymbol{\Omega}) = -(\kappa+\sigma)I(\boldsymbol{r},\boldsymbol{\Omega}) + \frac{\sigma}{4\pi}\int_{4\pi} I(\boldsymbol{r},\boldsymbol{\Omega}')\,d\Omega' + \kappa I_b(\boldsymbol{r}) \tag{1}$$

where $I(\boldsymbol{r},\boldsymbol{\Omega})$ is the radiation intensity, which is a function of position and direction; $I_b(\boldsymbol{r})$ is the intensity of blackbody radiation at the temperature of the medium; and κ and σ are the gray absorption and scattering coefficients of the medium, respectively.

If the surface Γ, bounding the region Λ, is assumed gray and emits and reflects diffusely, then the radiative boundary condition for Eq. (1) is given by

$$I(\boldsymbol{r},\boldsymbol{\Omega}) = \varepsilon I_b(\boldsymbol{r}) + \frac{\rho}{\pi}\int_{\hat{\boldsymbol{n}}\cdot\boldsymbol{\Omega}'<0} |\hat{\boldsymbol{n}}\cdot\boldsymbol{\Omega}| I(\boldsymbol{r},\boldsymbol{\Omega}')\,d\Omega' \tag{2}$$

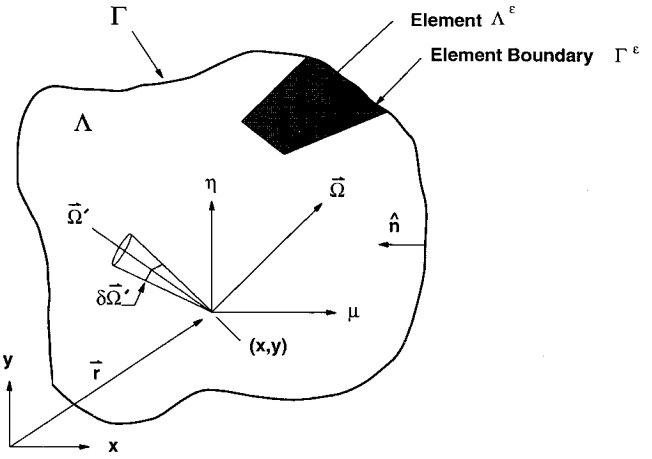

Fig. 1 Domain Λ and boundary Γ.

where $\boldsymbol{r}$ belongs to Γ, and Eq. (2) applies for $\boldsymbol{\Omega}\cdot\hat{\boldsymbol{n}} > 0$. $I(\boldsymbol{r},\boldsymbol{\Omega})$ is the intensity leaving a surface at a boundary condition location, ε is the surface emissivity, ρ is the surface reflectivity, and $\hat{\boldsymbol{n}}$ is the unit normal vector at the boundary location. Equations (1) and (2) represent the PV equations.

An even parity form of the RTE was derived in Fiveland and Jessee[12] following the work in Ref. 10:

$$-(\boldsymbol{\Omega}\cdot\nabla)\frac{1}{\beta}(\boldsymbol{\Omega}\cdot\nabla)\psi(\boldsymbol{r},\boldsymbol{\Omega}) = -\beta\psi(\boldsymbol{r},\boldsymbol{\Omega}) + \frac{\sigma}{4\pi}\int \psi(\boldsymbol{r},\boldsymbol{\Omega}')\,d\Omega' + \kappa I_b(\boldsymbol{r}) \tag{3}$$

This second-order equation has been shown to be positive definite and self-adjoint.[11] The corresponding boundary conditions are

$$-(1/\beta)(\boldsymbol{\Omega}\cdot\nabla)\psi(\boldsymbol{r},\boldsymbol{\Omega}) + \psi(\boldsymbol{r},\boldsymbol{\Omega}) = \varepsilon I_b(\boldsymbol{r}) + (1-\varepsilon)[q(\boldsymbol{r})/\pi] \tag{4a}$$

for $\boldsymbol{\Omega}\cdot\hat{\boldsymbol{n}} > 0$, and

$$(1/\beta)(\boldsymbol{\Omega}\cdot\nabla)\psi(\boldsymbol{r},\boldsymbol{\Omega}) + \psi(\boldsymbol{r},\boldsymbol{\Omega}) = \varepsilon I_b(\boldsymbol{r}) + (1-\varepsilon)[q(\boldsymbol{r})/\pi] \tag{4b}$$

for $\boldsymbol{\Omega}\cdot\hat{\boldsymbol{n}} < 0$, where $\boldsymbol{r}$ belongs to Γ.

Discrete-Ordinate Equations

The PV- and EP-RTEs—Eqs. (1) and (2) and Eqs. (3), (4a) and (4b), respectively—are replaced by a discrete set of equations for a finite number of directions $\boldsymbol{\Omega}_m$, and each integral is replaced by a quadrature. For the PV formulation, the resulting discrete ordinate equations are

$$(\boldsymbol{\Omega}_m\cdot\nabla)I(\boldsymbol{r},\boldsymbol{\Omega}_m) = -\beta I(\boldsymbol{r},\boldsymbol{\Omega}_m) + \frac{\sigma}{4\pi}\sum_{k=1}^{M} w_k I(\boldsymbol{r},\boldsymbol{\Omega}_k) + \kappa I_b \tag{5}$$

while for the EP formulation, the discrete ordinate equations are

$$-(\boldsymbol{\Omega}_m\cdot\nabla)\frac{1}{\beta}(\boldsymbol{\Omega}_m\cdot\nabla)\psi(\boldsymbol{r},\boldsymbol{\Omega}_m) = -\beta\psi(\boldsymbol{r},\boldsymbol{\Omega}_m) + \frac{\sigma}{4\pi}\sum_{k=1}^{M/2} w_k\psi(\boldsymbol{r},\boldsymbol{\Omega}_k) + \kappa I_b \tag{6}$$

where w_k is the weight corresponding to the incoming direction $\mathbf{\Omega}_k$. For a Cartesian geometry

$$\mathbf{\Omega}_m \cdot \nabla = \mu_m \frac{\partial}{\partial x} + \eta_m \frac{\partial}{\partial y} + \xi_m \frac{\partial}{\partial z} \tag{7}$$

where the values μ_m, η_m, and ξ_m are the direction cosines of $\mathbf{\Omega}_m$.

Direction Cosines and Corresponding Weights

The common approach in solving the DO equations is to use the S_n approximation.[4,5] This results in $n(n + 2)$ discrete directions. The ordinate values are symmetric and the weights sum to 4π. These sets are constructed to be invariant under any 90-deg rotation and to satisfy a number of key moments of the radiative intensity: 1) zeroth moment full-range $0 \le \theta \le \pi$, $0 \le \phi \le 2\pi$; 2) first moment half-range $0 \le \theta \le \pi/2$, $0 \le \phi \le 2\pi$; and 3) first moment full-range $0 \le \theta \le \pi$, $0 \le \phi \le 2\pi$.

The direction cosines and weights for the S_n approximations are listed in Refs. 4 and 5. An advantage of the S_n approximations is that they satisfy the key moments. Nevertheless, for $n > 12$, unrealistic negative weights may occur.

Other strategies may be used in selecting ordinates and weights. One such method is termed the PCA approximation. Briggs[18] showed that this approximation can "mitigate" the ray effects of the standard S_n approximation for the even parity equations. In the present work, the PCA approximation was extended and only applied to the primitive variable equations. The total solid angle (4π sr) is subdivided into a set of M, nonoverlapping, discrete solid angles, ($\Delta\Omega_m$: $m = 1, \ldots M$). The intensity I is assumed constant within each solid angle, and the governing RTE is integrated angularly over each respective solid angle. The resulting RTE is identical to Eq. (5) with the following substitutions:

$$\zeta_m = \frac{1}{w_m} \int_{\Delta\Omega} \xi \, d\mathbf{\Omega} \tag{8}$$

$$w_m = \int_{\Delta\Omega} d\mathbf{\Omega} \tag{9}$$

where ζ represents the direction cosines: μ, η, and ξ. Following the practice in Ref. 18, the total solid angle is divided uniformly in the ϕ and θ directions. The number of divisions are denoted by N_ϕ and N_θ, and the specific PCA approximation is denoted by $N_\phi \times N_\theta$. A similar angular approximation has recently been used by others.[15,16]

Although the PCA approximations mitigate ray effects, the method of selecting the directions does not insure that the key moments are satisfied. In fact, only the zeroth moment is guaranteed to be satisfied. Errors, sometimes as large as 20%, are generally present in the first moment, which is so important in predicting wall heat flux and consequently temperature. However, experience has shown that as the angular discretization is increased, errors in the higher moments are decreased.

Control Volume Finite Element Method

The governing equations are discretized spatially using the control volume finite element method,[20] which is also known as the subdomain weighted residual method.[21] In the weighted residual method,[22] the weighted governing partial differential equation is integrated over the entire domain of interest, and the result is set to zero:

$$\int_\Lambda w \text{ (governing equation) } d\Lambda = 0 \tag{10}$$

where the term "governing equation" in Eq. (10) denotes Eq. (5) or (6), and w denotes an as yet unspecified set of weight functions.

The EP equations are first discretized, since the derivation is more involved than the corresponding PV derivation, and the PV form can be inferred from the EP result. Equation (10) with Eq. (6) can be integrated by parts to obtain a "weak" form of the governing equation:

$$\int_\Lambda \nabla \cdot w\mathbf{\Omega} \left(\frac{1}{\beta} \nabla \cdot \mathbf{\Omega} \psi_m \right) d\Lambda - \int_\Lambda \nabla w \cdot \mathbf{\Omega} \left(\frac{1}{\beta} \nabla \cdot \mathbf{\Omega} \psi_m \right) d\Lambda - \int_\Lambda w\beta\psi_m \, d\Lambda + \int_\Lambda w S_m \, d\Lambda = 0 \tag{11}$$

where $m = 1, \ldots M/2$ are the discrete ordinate directions. The term S_m in Eq. (11) denotes sources from emission and in-scattering.

Green's theorem may be used on the first term of Eq. (11) to obtain

$$\int_\Gamma w\mathbf{\Omega} \left(\frac{1}{\beta} \nabla \cdot \mathbf{\Omega} \psi_m \right) \cdot \hat{n} \, d\Gamma - \int_\Lambda \nabla w \cdot \mathbf{\Omega} \left(\frac{1}{\beta} \nabla \cdot \mathbf{\Omega} \psi_m \right) d\Lambda - \int w\beta\psi_m \, d\Lambda + \int w S_m \, d\Lambda = 0 \tag{12}$$

Applying the subdomain method, the computational domain is subdivided into a number of elements as shown in Fig. 2, with the control volume surfaces defined by element midlines. This procedure creates a control volume for each node. Equation (12) is applied to each discrete control volume with w restricted to a set of functions that are unity within the control volume and zero in the remainder of the domain:

$$w \in (w_i, \quad i = 1, \ldots, N) \tag{13a}$$

$$w_i = 1 \quad \text{inside} \quad \Lambda_i$$

$$= 0 \quad \text{outside} \quad \Lambda_i \tag{13b}$$

For a given control volume, Eq. (12) is reduced to

$$\int_{\Gamma_i} \mathbf{\Omega} \left(\frac{1}{\beta} \nabla \cdot \mathbf{\Omega} \psi_m \right) \cdot \hat{n} \, d\Gamma - \int_{\Lambda_i} \beta\psi_m \, d\Lambda + \int_{\Lambda_i} S_m \, d\Lambda = 0 \tag{14}$$

Equation (14) essentially states that the net flux into the control volume exactly balances the sum of sinks due to extinction and sources due to emission and in-scattering.

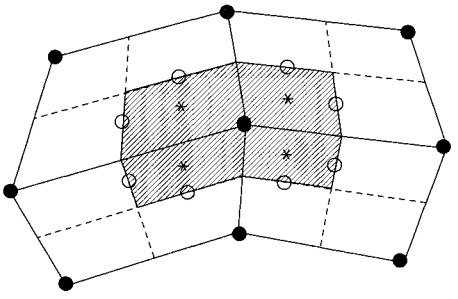

Fig. 2 Cluster of elements defining a control volume.

A control volume equation for the PV formulation follows from the previous methodology and the analogy between Eqs. (1) and (3):

$$-\int_{\Gamma_i} I_m \boldsymbol{\Omega}\cdot\hat{\boldsymbol{n}}\, d\Gamma - \int_{\Lambda_i} \beta I_m\, d\Lambda + \int_{\Lambda_i} S_m\, d\Lambda = 0 \quad (15)$$

Equations (14) and (15) are the integral representations of the even parity and primitive variable, discrete ordinates equations, respectively.

Spatially discrete forms of the equations are obtained by assuming some variation of the dependent variables and by numerically evaluating the spatial integrals. For the EP equations, the variation across each element is described with bilinear shape functions[23]:

$$\boldsymbol{r} = \sum_j^N N_j \boldsymbol{r}_j \qquad \psi_m = \sum_j^N N_j \psi_{jm} \quad (16)$$

The substitution of Eq. (16) into Eq. (14) provides N integral equations for each of the discrete ordinate directions. The integrals in Eq. (14) are recast into a discrete form by evaluating them at integration points, located as shown in Fig. 2. The discrete EP equations may be written symbolically as

$$a_{ijm}\psi_{jm} = S_{im} \quad \text{for} \quad m = 1, \ldots M/2 \quad (17)$$

For a given angular approximation, the EP formulation requires half the number of directions as the PV formulation because forward and reverse directions have been previously collapsed in the EP derivation.

For the first-order, PV equations, special treatments were required in the spatial representation of the dependent variable to provide positive, nonoscillatory solutions. First, the incident energy and radiant intensity in the divergence of the heat flux and the in- and out-scattering terms were assumed constant over respective volumes. Secondly, a bounded, second-order differencing scheme—the MINMOD scheme of Roe[19]—was applied to the transport term. The MINMOD scheme provides a highly accurate spatial differencing method, while eliminating oscillations and negative intensities that are characteristic of the diamond difference scheme. By using the above practices with Eq. (15), the following discrete PV equations are obtained:

$$a_{ijm}I_{jm} = S_{im} \quad \text{for} \quad m = 1, \ldots M \quad (18)$$

Solution Methods

The discretized even parity and primitive variable equations are represented by Eqs. (17) and (18), respectively. In the present work, each direction was solved independently. As a result, global iterations were necessary to include the source term and boundary conditions. The source term and wall heat fluxes were calculated based on the solution from the previous global iteration, and then a system of equations was solved for each ordinate direction. Global iterations continued until convergence was obtained. For the discrete EP equations, a direct solver was applied to the linear system of equations for each direction. Other solvers specifically designed for the banded matrices would speed calculations but were not used in the present work. For the discrete PV equations, the linear systems were solved by first reordering the equations based upon position of the respective nodes relative to the ordinate direction (i.e., upstream nodes were ordered first). This reordering procedure produces upper triangular coefficient matrix. Back substitution was then used to efficiently solve the system of equations.

Results

To compare the various formulations of the discrete ordinates method, three cases were examined: 1) absorbing medium in a black, rectangular enclosure; 2) scattering medium in a black/gray, rectangular enclosure; and 3) absorbing medium in a black circular enclosure. Predictions were made using the four basic formulations as shown in Table 1. Several S_n and PCA approximations were applied to the PV-CVFEM formulation.

For each case, the wall emissivity and absorption and scattering coefficients were assumed constant and spatially uniform. Convergence was measured using the change in the incident energy. Iterations were continued until the change in incident energy was less than 0.01%. For the cases considered, the balance between energy absorbed in the volume and the net surface flux matched to seven digits. Results are presented using nondimensional values; net wall heat fluxes and radiant intensities are normalized using a characteristic emissive power, whereas coordinate directions are normalized with a characteristic length.

Black Rectangular Enclosure with an Absorbing Medium

The discrete ordinates method was applied to a two-dimensional, rectangular enclosure with cold, black walls and a purely absorbing medium maintained at an emissive power of unity.[3,12] This enclosure is shown in Fig. 3 and is a special case of the geometry depicted in Fig. 1. This geometry was chosen since an exact solution is available.[3,24] Results are presented for 10 × 10 discretizations.

In Fig. 4, the net wall heat flux is predicted for absorption coefficients κ of 0.1, 1, and 10. Results for the different discrete ordinates solutions are compared to the exact solution. PV solutions compare well with the exact solution for all absorption coefficients. The shapes of the profiles at large and small absorption coefficient are captured. The PV-CV solutions were obtained using the diamond difference scheme, except for κ of 10. The step scheme was applied for κ of 10, because the diamond difference scheme produced nonphysical, oscillatory solutions. In contrast, the PV-CVFEM formulation with the MINMOD scheme produced no oscillations, even for the high absorption coefficient.

In Fig. 4, EP solutions compare well with the exact solution for small absorption coefficients, but as κ increases, the accuracy of the EP solutions degrades. Neither EP solution is able to correctly predict the trends of the exact solution for κ of 10. The absorption coefficient of 10 provides a photon mean free path [$\lambda = (1/\kappa)$] on the same order of magnitude as the characteristic element size for the 10 × 10 discretiza-

Table 1 Description of various discrete ordinates formulations

Name	Order of equations	Spatial differencing method	Angular differencing method	Reference
PV-CV	PV	CV/DD	S_n	3
PV-CVFEM	PV	CVFEM/MINMOD[19]	S_n, PCA	Present study
EP-FEM	EP	FEM/BL	S_n	12
EP-CVFEM	EP	CVFEM/BL	S_n	Present study

Note: CV = control volume method. DD = diamond difference. FEM = finite element method. BL = bilinear basis functions.

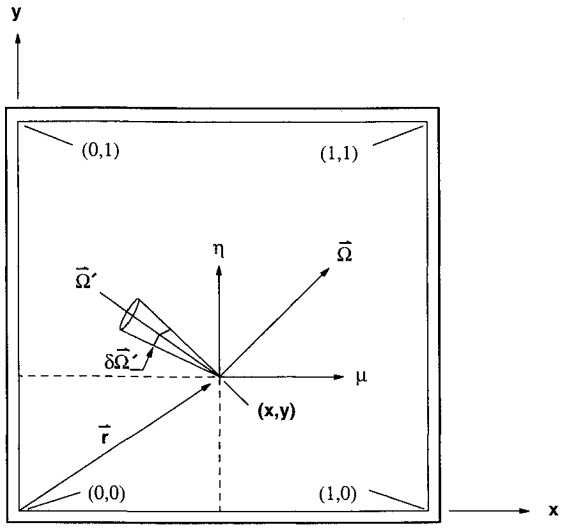

Fig. 3 Rectangular problem domain Λ and boundary Γ.

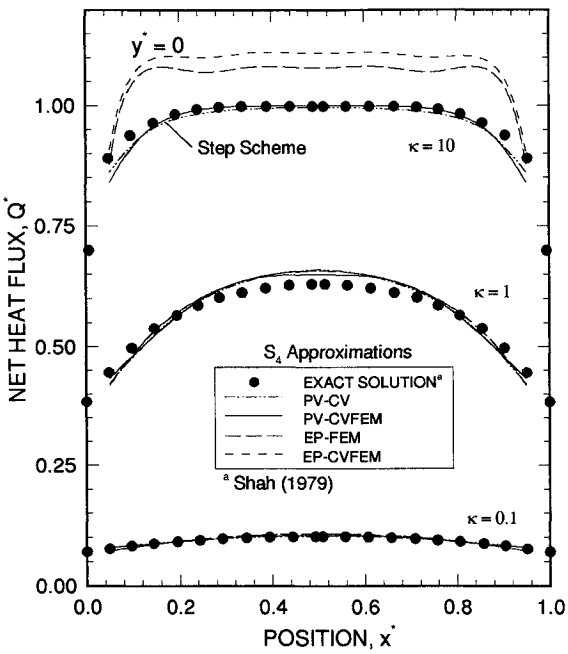

Fig. 4 Net wall heat flux in an enclosure with cold, black walls and a purely absorbing medium.

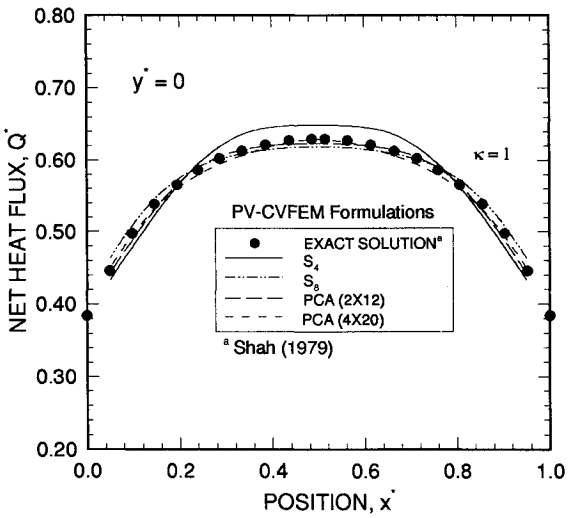

Fig. 5 Net wall heat flux profiles for various angular approximations for a purely absorbing medium.

tion. As a consequence, bilinear elements were unable to capture the exponential nature of the solution within the optical layer close to the boundary surface for the second-order EP equation.[12]

For the PV-CVFEM formulation, Fig. 5 shows a comparison of two angular discretization schemes: 1) the standard S_n approximation and 2) the PCA approximation.[18] All results are for an absorption coefficient of unity. The figure shows results for the S_4 and S_8 approximations, and for 2 × 12 and 4 × 20 PCA approximations. The 2 × 12 and 4 × 20 PCA approximations involve the same number of directions as the S_4 and S_8 approximations, respectively. Although the S_4 approximation is within 5% of the exact solution, the S_8 approximation captures the shape and magnitude of the exact solution (<1%); however, the S_8 solution requires more than three times the computational work of the S_4 solution. The 2 × 12 PCA approximation is nearly equal to the S_8, but only requires the computational work of the S_4 solution.

Pure Scattering in Black/Gray, Rectangular Enclosures

Radiative transfer in a square enclosure with black and gray walls and an isotropically scattering medium was studied. This geometry has been analyzed before,[3,12,25] and serves as a good benchmark for the discrete ordinates formulations. For the two-dimensional rectangular geometry, the lower wall ($y^* = 0$) has an emissive power of unity, and the other walls have zero emissive power. Enclosures with wall emissivities of 0.1, 0.5, and 1.0 were considered. Ten to fifteen iterations were required to achieve converged solutions for emissivities of 1.0. Figures 6 and 7 display the net wall heat flux and incident energy for the S_4 discrete ordinate solutions.

Figure 6 shows the predicted net wall heat flux for several discrete ordinate solutions compared to the exact zone solution of Ratzel and Howell.[25] For an enclosure with black walls, the EP solutions are not as accurate as either the PV-CVFEM formulation or the PV formulation,[4] using the quadratures from Ref. 5. As wall emittance decreases, the EP solutions approach the PV solution. Both EP solutions have the same characteristics: they predict the heat flux in the center of the boundary walls, but are unable to predict profile near the corners.

Figure 7 shows three profiles of incident energy at $x^* = 0.1$, 0.3, and 0.5 for the black wall case. The predictions from

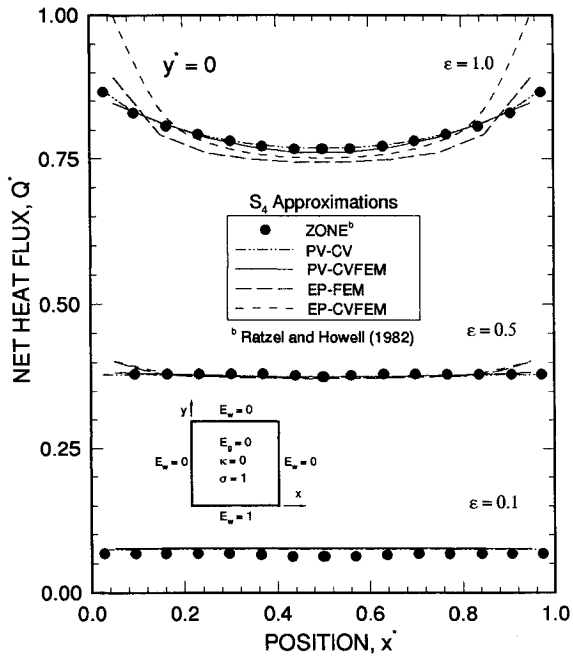

Fig. 6 Net wall heat flux in a square enclosure with scattering medium.

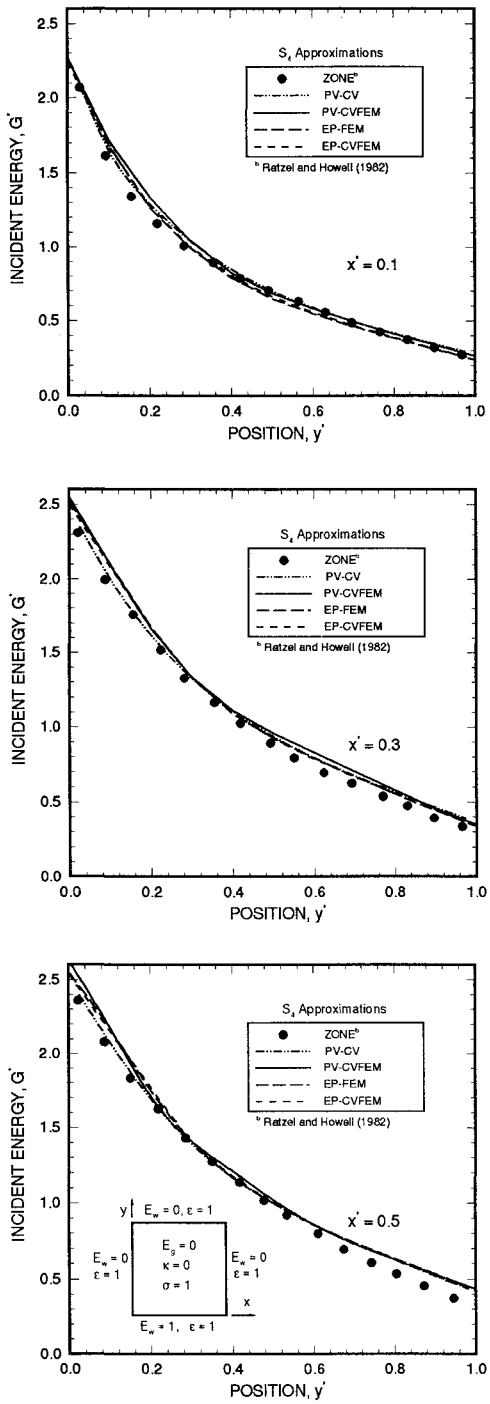

Fig. 7 Incident radiant energy in a square enclosure with scattering medium.

the various formulations of the discrete ordinates method are compared to the zone data.[25] All DO solutions compare reasonably well with the zone method. In contrast to the heat flux profiles with wall emissivity of unity as shown in Fig. 6, the predicted incident energy profiles of the EP and PV formulations are very similar. At $x^* = 0.5$ and $y^* = 0.5$, all solutions satisfy the exact solution,[26] producing an incident energy of unity.

The EP solutions are more sensitive to mesh spacing and optical properties. This is due to the second-order, even parity equation, which has Marshak-type boundary conditions for the transformed set. While both the PV and EP equations exhibit singular perturbation character (loss of the highest order derivative) with large extinction coefficient, the EP equation is most affected. The use of FEM or CVFEM has little effect on solution accuracy. Fiveland and Jessee[12] showed that improved accuracy could be obtained by using a nonuniform mesh spacing with elements concentrated in the near-wall region. The use of the nonuniform mesh spacing with the EP-CVFEM formulation has the same effect as described in Ref. 12.

Figure 8 displays predictions from the PV-CVFEM formulation using a variety of angular approximations. Results are given for a wall emissivity of unity. The figure shows that all angular approximations produce nearly the same heat flux profile at the bottom wall. These predictions contrast the these predictions for the absorption case as shown in Fig. 5. Variations in the profiles are very evident for the absorbing media, whereas no significant differences are indicated in the predictions for the scattering media. These results are expected since ray effects are generally more pronounced for purely absorbing media.

Circular Enclosure with an Absorbing Medium

Radiative transfer in a circular enclosure with black, cold walls and an absorbing medium was considered.[2] This problem is essentially one-dimensional, and serves as a good benchmark because exact solutions are available. Also, the example demonstrates the capability of the PV-CVFEM formulation for a curved wall geometry. Predictions were made with the PV-CVFEM formulation using a number of angular discretizations. Figure 9 shows a finite element grid for the

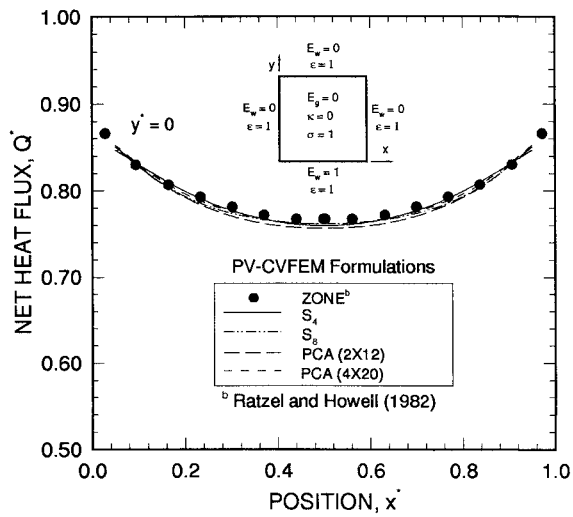

Fig. 8 Net wall heat flux profiles for various angular approximations for a purely scattering medium.

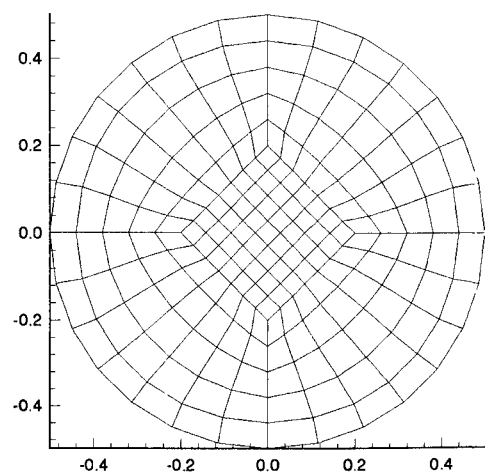

Fig. 9 Computational grid for circular test case.

Table 2 Net wall heat flux for circular geometry for a range of optical thicknesses ($\tau = \kappa R$)

τ	Exact[2]	S_6	S_8	PCA 4 × 20
0.1	0.1770	0.1762	0.1748	0.1753
0.2	0.3172	0.3160	0.3123	0.3129
0.5	0.5960	0.5948	0.5871	0.5824
1	0.8143	0.8149	0.8063	0.7926
2	0.9458	0.9482	0.9401	0.9215
5	0.9923	0.9923	0.9842	0.9651

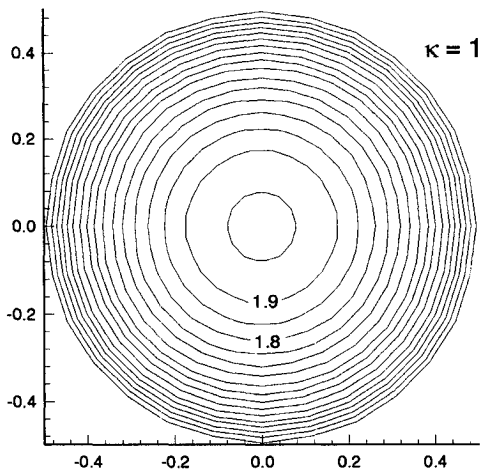

Fig. 10 Predicted incident energy for circular test case with S_6 approximation and $\kappa = 1$.

cylindrical geometry with a diameter of unity. The grid is composed of 189 elements.

Figure 10 shows a contour plot of incident energy for the S_6 approximation with an absorption coefficient of unity. The predicted incident energy is nearly symmetrical. Slight ray effects are present, but are not noticeable in the contour plot. Table 2 lists the exact[2] and predicted wall heat fluxes for a range of optical thicknesses. The predicted values are averages for the circumference of the enclosure. Due to ray effects, slight circumferential variations (<2%) were present in all predictions. The average heat fluxes of the S_n approximations agree better than those of the PCA approximation, but ray effects were less apparent in the PCA predictions. Overall, the predictions agree well with the exact solutions, even at high optical thicknesses.

Summary

Control volume based, finite element formulations have been presented for the PV and EP radiative transport equations. Solutions from the new formulations have been compared to 1) solutions from the primitive variable control volume formulation,[3] 2) solutions from the finite element even parity formulation,[12] and 3) exact solutions.

Predictions from the primitive variable formulations compare better with the exact solution than do the predictions from the even parity formulations. This included both absorption and scattering test enclosures for a range of optical properties and wall emissivities. The accuracy of the EP predictions degrades as the optical thickness and wall emissivity are increased.

Two angular discretization schemes were compared. The PCA approximations produced smaller ray effects compared to computationally equivalent S_n approximations; however, for the circular test case, the average wall heat flux was predicted more accurately with the S_n approximations. The merits of the PCA approximations remain to be proven for three-dimensional geometries and for anisotropically scattering media. Problems are expected since PCA approximations generally are not invariant under 90-deg rotations, and generally do not conserve moments higher than the zeroth.

The second-order accurate MINMOD differencing scheme overcomes many problems of the standard step, diamond difference, and exponential schemes. Second-order accuracy is obtained while insuring positive, nonoscillatory solutions. The scheme is applicable to both the cell-centered, control volume (CV) and the vertex-based CVFEM formulations.

Based on the present findings, future research should focus on the primitive variable equations. Of the PV formulations, the CVFEM is recommended since it is applicable to complex geometries. The family of bounded, higher-order differencing schemes—of which the MINMOD scheme is a member—holds promise for providing accurate, nonoscillatory solutions and should be further investigated.

References

[1]Viskanta, R., and Menguc, M. P., "Radiation Heat Transfer in Combustion Systems," *Progress in Energy and Combustion Science*, Vol. 13, No. 2, 1987, pp. 97–160.

[2]Modest, M. F., *Radiative Heat Transfer*, McGraw-Hill, New York, 1993.

[3]Fiveland, W. A., "Discrete-Ordinates Solutions of the Radiative Transport Equation for Rectangular Enclosures," *Transactions of the American Society of Mechanical Engineers, Journal of Heat Transfer*, Vol. 106, No. 4, 1984, pp. 699–706.

[4]Fiveland, W. A., "Three-Dimensional Radiative Heat Transfer Solutions by the Discrete-Ordinates Method," *Journal of Thermophysics and Heat Transfer*, Vol. 2, No. 4, 1988, pp. 309–316.

[5]Fiveland, W. A., and Jamaluddin, A. S., "Three-Dimensional Spectral Radiative Heat Transfer Solutions by the Discrete Ordinates Method," *Journal of Thermophysics and Heat Transfer*, Vol. 5, No. 3, 1991, pp. 335–339.

[6]Kim, T. K., and Lee, H., "Effect of Anisotropic Scattering on Radiative Heat Transfer in Two-Dimensional Rectangular Enclosures," *International Journal of Heat and Mass Transfer*, Vol. 31, No. 8, 1988, pp. 1711–1721.

[7]Jamaluddin, A. S., and Smith, P. J., "Predicting Radiative Transfer in Axisymmetric Cylindrical Enclosures Using the Discrete Ordinates Method," *Combustion Science and Technology*, Vol. 62, Nos. 4–6, 1988, pp. 173–186.

[8]Lathrop, K. D., and Carlson, B. G., "Discrete Ordinates Angular Quadrature of the Neutron Transport Equation," Los Alamos Scientific Lab. Rept., LASL-3186, Los Alamos, NM, 1965.

[9]Truelove, J. S., "Discrete-Ordinates Solutions of the Radiation Transport Equation," *Transactions of the American Society of Mechanical Engineers, Journal of Heat Transfer*, Vol. 109, No. 4, 1988, pp. 1048–1051.

[10]Lewis, E. E., and Miller, W. F., *Computational Methods of Neutron Transport*, Wiley, New York, 1984.

[11]Kaplan, S., and Davis, J. A., "Canonical and Involuntary Transformations of the Variational Problems of Transport Theory," *Nuclear Science and Engineering*, Vol. 28, No. 1, 1967, pp. 166–176.

[12]Fiveland, W. A., and Jessee, J. P., "A Finite Element Formulation of the Discrete Ordinates Method for Multidimensional Geometries," *Journal of Thermophysics and Heat Transfer*, Vol. 8, No. 3, 1994, pp. 426–433.

[13]Carlson, B. G., and Lathrop, K. D., *Transport Theory—The Method of Discrete-Ordinates in Computing Methods in Reactor Physics*, edited by H. Greenspan, C. Kelber, and D. Okrent, Gordon and Breach, New York, 1968.

[14]Fiveland, W. A., "The Selection of Discrete Ordinate Quadratures Sets for Anisotropic Scattering," *Fundamentals of Radiation Heat Transfer*, 28th National Heat Transfer Conf., American Society of Mechanical Engineers HTD-Vol. 160, 1992, pp. 89–96.

[15]Chai, J. C., Lee, H. S., and Patankar, S. V., "Finite Volume Method for Radiation Heat Transfer," *Journal of Thermophysics and Heat Transfer*, Vol. 8, No. 3, 1994, pp. 419–425.

[16]Raithby, G. D., and Chui, E. H., "A Finite-Volume Method for Predicting a Radiant Heat Transfer in Enclosures with Participating Media," *Transactions of the American Society of Mechanical Engineers, Journal of Heat Transfer*, Vol. 112, No. 2, 1990, pp. 415–423.

[17]Chui, E. H., and Raithby, G. D., "Computation of Radiant Heat Transfer on a Nonorthogonal Mesh Using the Finite-Volume Method," *Numerical Heat Transfer*, Pt. B, Vol. 23, 1993, pp. 269–288.

[18]Briggs, L. L., Miller, W. F., and Lewis, E. E., "Ray-Effect Mitigation in Discrete Ordinate-Like Angular Finite Element Approximations in Neutron Transport," *Nuclear Science and Technology*, Vol. 57, No. 3, 1975, pp. 205–217.

[19]Harten, A., "High Resolution Schemes for Hyperbolic Conservation Laws," *Journal of Computational Physics*, Vol. 49, No. 3, 1983, pp. 357–393.

[20]Schneider, G. E., and Raw, M. J., "Control Volume Finite-Element Method for Heat Transfer and Fluid Flow Using Colocated Variables," *Numerical Heat Transfer*, Vol. 11, No. 4, 1987, pp. 363–390.

[21]Fletcher, C. A. J., *Computational Techniques for Fluid Dynamics*, Vol. II, Second ed., Springer Series in Computational Physics, Springer-Verlag, Germany, 1991.

[22]Crandall, S. H., *Engineering Analysis*, McGraw-Hill, New York, 1956.

[23]Zienkiewicz, O. C., and Taylor, R. L., *The Finite Element Method*, Vol. 1, 4th ed., McGraw-Hill, New York, 1989.

[24]Shah, N., "New Method of Computation of Radiation Heat Transfer in Combustion Chambers," Ph.D. Dissertation, Dept. of Mechanical Engineering, Imperial College of Science and Technology, Univ. of London, London, 1979.

[25]Ratzel, A. C., and Howell, J., "Two Dimensional Radiation in Absorbing-Emitting-Scattering Media Using the P-N Approximation," American Society of Mechanical Engineers Paper 82-HT-19, 1982.

[26]Crosbie, A. I., and Schrenker, R. G., "Exact Expressions for Radiative Transfer in a Three-Dimensional Rectangular Geometry," *Journal of Quantitative Spectroscopy and Radiative Transfer*, Vol. 28, No. 6, 1982, pp. 507–526.